PHYSICAL REVIEW D **84,** 084027 (2011)

Acoustic metric of the compressible draining bathtub

C. Cherubini and S. Filippi

Nonlinear Physics and Mathematical Modeling Lab, University Campus Bio-Medico, Via A. del Portillo 21, I-00128 Rome, Italy and International Center for Relativistic Astrophysics, University of Rome "La Sapienza", I-00185 Rome, Italy

(Received 20 July 2011; published 13 October 2011)

The draining bathtub flow, a cornerstone in the theory of acoustic black holes, is here extended to the case of exact solutions for compressible nonviscous flows characterized by a polytropic equation of state. Investigating the analytical configurations obtained for selected values of the polytropic index, it is found that each of them becomes nonphysical at the so called *limiting circle*. By studying the null geodesics structure of the corresponding acoustic line elements, it is shown that such a geometrical locus coincides with the acoustic event horizon. This region is characterized also by an infinite value of space-time curvature, so the acoustic analogy breaks down there. Possible applications for artificial and natural vortices are finally discussed.

DOI: 10.1103/PhysRevD.84.084027 PACS numbers: 47.40.−x, 04.20.−q, 47.40.Nm

I. INTRODUCTION

General Relativity (GR) deals with curved space-times of astrophysical interest. Recently the mathematical structure of this fundamental theory has been linked with the analog geometries (Analog Gravity) [1–3] emerging in nonrelativistic contexts of condensed matter physics, under the inspiration of the seminal theoretical works by Unruh [4,5]. The acoustic perturbations, both irrotational or not, for a nonrelativistic classical perfect fluid can be described as the dynamics of a real massless scalar field in a four dimensional Lorentzian manifold where the speed of sound plays the role of the speed of light.

A toy model called the draining bathtub [6] has been proposed some years ago in order to understand a possible black hole/white hole dynamics, and plenty different studies [7–14] have analyzed this simple system in search or analogies with GR. The draining bathtub is a steady planar flow with simple radial and tangential velocity components and constant density, pressure, and speed of sound. The extrusion of this plane flow on the z direction gives a simple model for a three dimensional vortex. Standard hydrodynamics arguments clearly show that this cannot be a solution of Euler's equation. In absence of external forces (as gravity) and for static configurations only in fact, pressure and density of the fluid can be both constant. If the fluid is in stationary motion with spatial velocity gradients, Bernoulli's theorem states that pressure cannot be constant in space. This means that a more realistic situation than the draining bathtub is necessary, possibly including compressibility which is the physical mechanism propagating acoustic disturbances. Because of the weak compressibility of ordinary fluids, we must extend our analysis to the realm of gas-dynamics then.

We have to point out, as a *caveat* given in Ref. [1], that the acoustic metrics in this more general case could allow sets of acoustic perturbations which, although initially small, may induce the development of shocks, possibly leading to additional technical complications as a weak-form formulation of hydrodynamics. We recall moreover that in the context of Analog Gravity, the de Laval nozzles have been the classical prototype adopted to numerically study compressible polytropic flows through the acoustic metric [15]. These configurations are extremely simplified reducing the problem to a $1 + 1$ transient dynamics on which extract linear sound waves, while perturbed vortices are intrinsically of $2 + 1$ or $3 + 1$ types, showing manifestly curvature effects to be taken into account.

We must remark moreover that while the original theoretical studies on acoustic black holes have pointed in favor of quantum condensates at low temperatures (so practically with zero viscosity) as appropriate experimental counterparts, what we want to study here is a classical nonviscous compressible flow. This is a classical gaseous system which, in presence of rotation, could describe in a first approximation macroscopic vortices commonly encountered in experiments. Clearly we could imagine to include in this treatment also large scale whirlpools as hurricanes, tornadoes or typhoons. In fact, although these are quite complicated systems of nature in which heat transfer and viscous effects play a prominent role, we may imagine to perform reasonable simplifications which could allow one to grasp some of their important physical aspects. In this spirit, we present in Fig. 1 a sketch of a sufficiently realistic whirlpool-type gaseous/fluid configuration (a) contrasted with the even more idealized one (b) as adopted in this article. A fluid is thought not to exist in the region inside the hole (what in a generic rotating fluid would be a sharp air-liquid interface), while in gaseous configurations this picture is less demarcated but still apparent. We must anticipate here that in the mathematical theory of gas dynamics, whose standard references are Courant and Friedrichs's volume [16] together with Von Mises's monograph on compressible flows [17] (both of these are followed in this article), the field equations automatically lead to a minimal critical radius (the so called *limiting* or *limit*

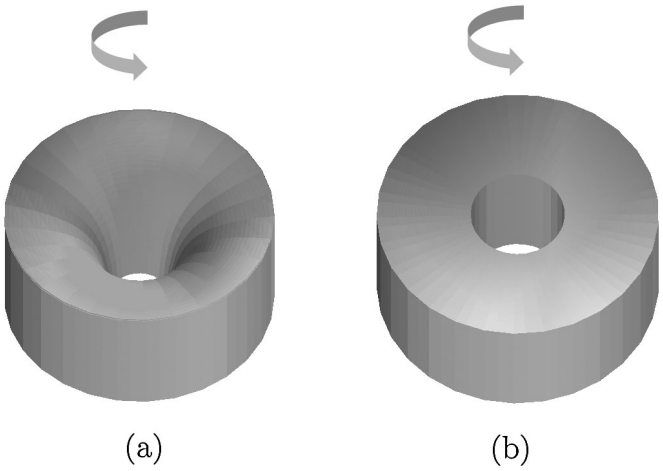

FIG. 1. Sketch of a somewhat realistic whirlpool-type fluid configuration (a) and of the even more idealized one (b) discussed in this article.

circle for the spiral flow discussed later) beyond which the solution results complex, and so are nonphysical. For this reason we have plotted a hole already in the (b) configuration. We shall neglect as a first approximation gravitational effects and as an additional idealization we shall moreover assume to observe a sufficiently thick slice of the configuration (b) far enough from the upper and lower interfaces in order to avoid any border effect. As we shall see later, the compressible fluid arrives at the last physical radius with a finite velocity. One may imagine then to cut and paste this outer solution with another inner more complicated but regular one. It would be possible in this case even to consider the acoustic metric formalism for a rotational flow along the lines of Ref. [18] adopting Clebsch's potential theory for Euler's equations [19–23]. On the other hand, the addition of the viscosity would result dramatic for the theoretical scheme adopted by inducing a breaking of the analog Lorentz invariance [6], and so it cannot be considered.

We will present now the structure of the article. After this introduction, we give in Sec. II the mathematical formulation which can permit us to obtain analytical solutions of Euler's equations. In Sec. III these solutions are framed in the context of analog space-times by studying possible event horizons, ergospheres, and curvature singularities. Finally in Sec. IV a general physical discussion of the results is presented.

II. INCOMPRESSIBLE AND COMPRESSIBLE POLYTROPIC DRAINING BATHTUB SOLUTIONS

As anticipated in the introduction, we want to model three-dimensional incompressible and compressible vortical gaseous/fluid geometries. In presence of gravity this is a complicated free boundary problem for the air-fluid interface. Free boundary problems still are not a well developed sector for analytical solution techniques [24] (while numerically they are well studied), so we must relax our initial conditions by assuming a flow which is well defined, *a priori*, on an entire cylindrical domain. The role of gravity is neglected in our treatment for the sake of simplicity, in order to make us possible to adopt separation of variables techniques and work with ordinary differential equations instead of partial differential ones.

We start studying then a time independent configuration in cylindrical coordinates (r, θ, z) assuming no t, z, and θ dependence of functions as well as $v_z = 0$. The problem then collapses from a three dimensional to a two dimensional one (but every $z =$ constant plane contains the same physics, so extruding back along z direction we can get a steady three dimensional plane motion). Assuming a purely radial dependence we can write

$$\begin{aligned} \rho &= \rho(r), \qquad & p &= p(r), \\ v_r &= v_r(r) \qquad & v_\theta &= v_\theta(r). \end{aligned} \tag{1}$$

The curl of this velocity field results in $\nabla \times \vec{v} = (\frac{dv_\theta}{dr} + \frac{v_\theta}{r})\hat{z}$, while its divergence is $\nabla \cdot \vec{v} = (\frac{dv_r}{dr} + \frac{v_r}{r})$. From these conditions we obtain the following field equations (mass and momentum conservation) [25]

$$v_r \frac{d\rho}{dr} + \rho \frac{dv_r}{dr} + \frac{v_r}{r}\rho \equiv \frac{1}{r}\frac{d}{dr}(\rho r v_r) = 0 \tag{2}$$

$$\rho v_r \frac{dv_r}{dr} + \frac{dp}{dr} - \frac{\rho v_\theta^2}{r} = 0 \tag{3}$$

$$\frac{\rho v_r}{r}\left(r\frac{dv_\theta}{dr} + v_\theta\right) = 0. \tag{4}$$

Equations (2) and (4) imply

$$v_\theta = \frac{B}{r}, \qquad v_r = \left(\frac{A}{r}\right)\frac{1}{\rho}, \qquad A, B \in \mathcal{R}. \tag{5}$$

This result leads to an irrotational flow except in the origin where the velocity field is not defined. We point out that in this flow the quantity $2\pi r v_\theta \equiv 2\pi B$ represents the constant circulation Γ on a circle of radius r around the origin. As expected for an irrotational flow, the circulation is equal for all circuits surrounding an ''obstacle'' (the inner region where, as we will see, the flow is not defined) [17]. Choosing $A > 0$ we have an outgoing flow (a source) while the case $A < 0$ gives a sink.

Inserting into Eq. (3) we finally obtain

$$\frac{A^2}{r^2\rho^2}\frac{d\rho}{dr} + \frac{A^2}{r^3\rho} + \frac{\rho B^2}{r^3} - \frac{dp}{dr} = 0. \tag{6}$$

In this flow, a supersonic regime occurs where the local Mach number $\mathcal{M}$ satisfies

$$\mathcal{M} \equiv \frac{v}{c_s} > 1, \qquad v = \sqrt{v_r^2 + v_\theta^2}, \qquad c_s^2 = \frac{dp(\rho)}{d\rho}, \tag{7}$$

where we have introduced the local speed of sound c_s [16]. The equality $\mathcal{M} = 1$ must define the sonic point while $\mathcal{M} < 1$ leads to subsonic flows instead. We can address now the analysis of several different types of flows associated with this formulation.

A. Incompressible flows

Assuming incompressibility, i.e. $\rho(r) = \rho_0 = \text{constant}$, we obtain that $v_r = \frac{A}{\rho_0}\frac{1}{r}$ and this leads, as required, to $\text{div}\vec{v} = 0$. From Eq. (3) we obtain

$$p(r) = p_\infty - \frac{(A^2 + \rho_0^2 B^2)}{2\rho_0 r^2}, \tag{8}$$

where p_∞ is the constant value of pressure present at infinite distance from the origin. At a finite critical radius

$$r_c = \sqrt{(A^2 + \rho_0^2 B^2)/(2\rho_0 p_\infty)} \tag{9}$$

pressure vanishes and beyond this point it changes sign so that the physical solution terminates here.

The original draining bathtub configuration [6], characterized by

$$v_r = \frac{\tilde{A}}{r}, \qquad v_\theta = \frac{\tilde{B}}{r}, \qquad \tilde{A}, \tilde{B} \in \mathcal{R}, \qquad \rho = \text{constant},$$
$$p = \text{constant}, \qquad c_s = \text{constant} \tag{10}$$

is not a solution of Euler's equations. It can be linked however to the incompressible configuration just found by neglecting the radial dependent term of the pressure. Because of the r^{-2} behavior, this is a meaningful operation sufficiently far from the origin and assuming, moreover, a constant speed of sound c_s. We stress that perturbative wave propagation in such a configuration is meaningful only relaxing the initial condition of incompressibility to a slightly compressible fluid [25] (necessary condition for having acoustic perturbations). Strictly speaking in fact, incompressible perturbations of an incompressible fluid cannot give sound waves, which by definition require density variations of the medium. In this case then, from the equation of state $p - p_0 = K(\rho - \rho_0)$ with p_0, ρ_0, and K (the latter very large) being real constants, we get from usual formula $c_s^2 = \frac{dp(\rho)}{d\rho}|_{\rho=\rho_0}$ that the constant sound speed results into $c_s = \sqrt{K}$. It appears more reasonable then to assume always the possibility of compressibility, even small. This is done in the next pages.

B. Compressible flows for finite values of the polytropic index n

If no incompressibility constraint is assumed, we must provide an equation of state which in our case will be the polytropic one i.e. $p = k\rho^{1+(1/n)}$ with positive real constants k and n. The limit $n \to 0$ is pathological, but standard manipulations, commonly adopted in astrophysics as an example [26,27], show that it corresponds to the incompressible case already studied. In the general n case, the local sound speed of acoustic disturbances for polytropic configurations will be given by

$$c_s^2 = \frac{dp(\rho)}{d\rho} \equiv k\left(1 + \frac{1}{n}\right)\rho^{1/n}. \tag{11}$$

In this case, Eq. (6) becomes

$$\left[\left(\frac{n+1}{n}\right)k\rho^{1/n} - \frac{A^2}{r^2\rho^2}\right]\frac{d\rho}{dr} - \frac{A^2}{r^3\rho} - \frac{B^2\rho}{r^3} = 0, \tag{12}$$

whose solution for $0 < n < +\infty$, obtained through standard symmetry methods for ordinary differential equations (see Appendix for details), is given by

$$k(n+1)\rho^{1/n} + \frac{A^2}{2r^2\rho^2} + \frac{B^2}{2r^2} = C_1, \tag{13}$$

where C_1 is a constant of integration. Relation (13) from Eq. (11), can be written as

$$c_s^2 \equiv k\left(1 + \frac{1}{n}\right)\rho^{1/n} = \frac{1}{n}\left(C_1 - \frac{A^2}{2r^2\rho^2} - \frac{B^2}{2r^2}\right) \geq 0 \tag{14}$$

which requires $C_1 > 0$ in order to have a real sound speed.

The solution can be rewritten explicitly in the plane $\rho - r$ by isolating in Eq. (13) the r^2 quantity, taking the square root and choosing the positive radius solution (the physical one) only, i.e.

$$r \equiv r(\rho) = \frac{1}{\rho}\sqrt{\frac{A^2 + \rho^2 B^2}{2[C_1 - k(n+1)\rho^{1/n}]}}. \tag{15}$$

This is an highly transcendent relation showing that the origin $r = 0$, by assuming a non-negative and finite density ρ for physical reasons, can never be reached, i.e. the configuration becomes nonphysical at a certain critical radius r_c. The inversion of the relation (13) in the more useful form $\rho = \rho(r)$ is nontrivial except for specific values of the polytropic index (specifically $n = 1/2,\ 1,\ +\infty$).

Although we could approach the problem numerically, we shall try to use analytical methods only in view of the acoustic metric formalism manipulations. We point out that in the case of $A = 0$ (no radial flow) the analytical solution of the problem is simply

$$\rho(r) = \left[C_1 - \frac{B^2}{2(n+1)kr^2}\right]^n, \tag{16}$$

which becomes nonphysical again at a finite radius $r_c = B/\sqrt{2kC_1(n+1)}$. The other case with $B = 0$ and $A \neq 0$ is not different qualitatively from the most general case so we shall not address it further.

C. The case $n = 1/2$

In this case Eq. (13) gives a fourth order equation in ρ which can be solved giving four branches for $\rho = \rho(r)$.

Moreover for the sound speed we have now that $c_s^2 = 3k\rho^2$. Two physical branches of the solution only must exist because the remaining ones refer to negative densities and consequently must be disregarded. We remain then with the two solutions $\rho_\pm$ given by

$$\rho_\pm = \sqrt{\frac{C_1}{3k} - \frac{B^2}{6kr^2} \pm \frac{\sqrt{(B^2 - 2C_1r^2)^2 - 12kA^2r^2}}{6kr^2}}. \quad (17)$$

In the expression just derived the parameters A and B enter quadratically so the solution will be the same for any signs choice of these.

In Eq. (17) the two different roots however have a very different physical meaning. The solution with the plus sign ρ_+ represents in fact a flow which is subsonic but becomes supersonic at a specific radius. This solution starts at rest (i.e. $\vec{v} = 0$) at radial infinity with density $\rho_+^\infty = \sqrt{\frac{2C_1}{3k}}$ which monotonically decreases going towards the configuration up to a finite radius r_c, discussed below, where the solution physically terminates but the density remains finite. In parallel the Mach number for this configuration is zero at radial infinity, increases going towards the center, becomes unity at a specific radius r_s, and is supersonic at the final physical radius r_c (we call this the *mixed* case).

The other solution ρ_- instead has a different meaning. It is associated with a flow with zero asymptotic density which monotonically increases going towards the center of the configuration up to a finite value reached at r_c. In this case however the Mach number at infinity is infinite and decreases monotonically towards the center arriving to a last finite bigger than one value; this is a flow which is always supersonic with asymptotic value $v^\infty = \sqrt{2C_1}$. The critical and sonic radii can be even found analytically. A rapid check shows that solution (17) becomes complex for radii smaller than

$$r \equiv r_c = \sqrt{\frac{B_1^2}{2C_1} + \frac{3kA^2}{2C_1^2} + \frac{\sqrt{3k}|A|\sqrt{3kA^2 + 2B^2C_1}}{2C_1^2}}. \quad (18)$$

Focusing on the ρ_+ branch, in the limit $r \to r_c$ the associated Mach number results in $\mathcal{M} \to \mathcal{M}_c \equiv (1 + \frac{2B^2C_1}{3kA^2}) > 1$, so as anticipated, the ρ_+ solution ends supersonic. On the other hand at analytical sonic radius

$$r_s = \frac{\sqrt{3kA^2 + B^2C_1}}{C_1} \quad (19)$$

the Mach number of ρ_+ reaches value $\mathcal{M} = 1$. The analytical radius for the sonic point r_s is larger than the last physical radius r_c. In the limit $r \to r_c$, using simple algebra one can show that the ratio $|v_r/c_s| \to 1$; as we will see, in analogy with Visser's study this corresponds to the acoustic event horizon.

We point out finally that in the limit $B \to 0$ (purely radial flows) we have that $r_c \to r_s$, so the solution physically ends at the sonic radius. The solution given by

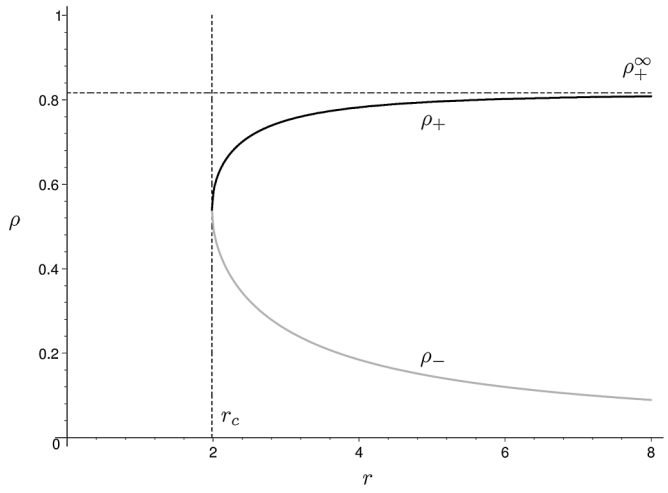

FIG. 2. Density ρ versus radius r plot for the $n = 0.5$ solution with parameters $A = B = k = C_1 = 1$. The solution has two branches. One with the plus sign ρ_+ (black solid line) represents a flow which is subsonic but becomes supersonic at a specific radius. It starts with finite asymptotic density ρ_+^∞ and decreases monotonically up to a critical radius r_c. The other minus sign solution ρ_- (grey solid line) is associated with a flow which has zero asymptotic density but nonzero asymptotic radial velocity $\sqrt{2C_1}$, which monotonically increases going out the center of the configuration up to a finite value at the last physical radius r_c. The plot is the same in the case of the ingoing sink-type flux with $A = -1$.

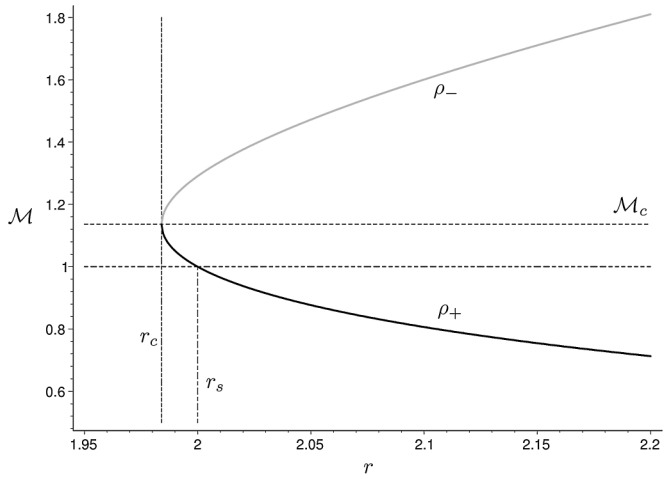

FIG. 3. Local Mach number $\mathcal{M}$ versus radius r plot for the $n = 0.5$ solution with parameters $A = B = k = C_1 = 1$. There are two branches. The solution with the plus sign ρ_+ represents a flow which is essentially subsonic and at rest at spatial infinity but becomes supersonic at a specific radius r_h (sonic point with $\mathcal{M} = 1$) up to a last physical radius r_c. The ρ_- branch instead is always supersonic with infinite Mach number at radial infinity. The plot is the same in the case of the ingoing sink-type flux with $A = -1$.

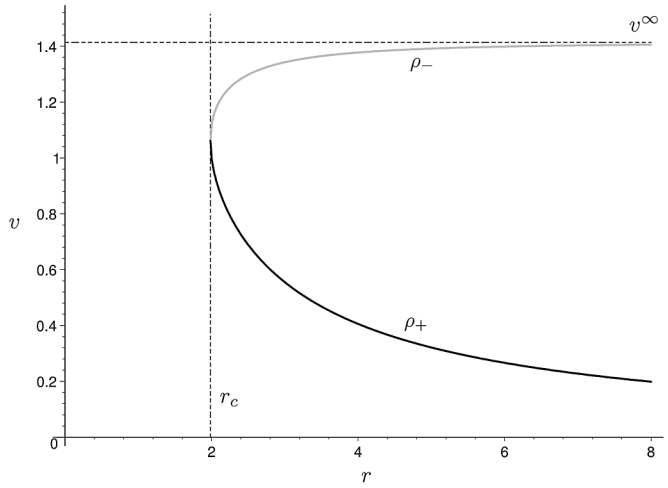

FIG. 4. Velocity magnitude $v = |\vec{v}|$ versus radius r plot for the $n = 0.5$ solution with parameters $A = B = k = C_1 = 1$. There are two branches. The solution with the plus sign ρ_+ is in black while the ρ_- one is in gray. The plot is the same for $A = -1$.

Eq. (17) is shown in Fig. 2 for a generic choice of parameters $A = B = k = C_1 = 1$ (other different nonzero choices lead to similar results). Taking the $A < 0$ case (the sink) plots as anticipated are not changed. In Fig. 3 instead for the same parameter's choice we plot the Mach number versus the radius for the same solution. In Fig. 4 we have the magnitude of velocity $v = |\vec{v}|$, and in Fig. 5 the radial dependence of local sound speed. In Fig. 6 instead we draw the field vectors for parameters $B = k = C_1 = 1$ in the case: (a) ρ_+ and $A = -1$, (b) ρ_+ and $A = 1$, (c) ρ_- and $A = -1$, and (d) ρ_- and $A = 1$. Finally in Fig. 7 we plot the field lines and arrow plot for the ρ_+ solution with parameters $B = k = C_1 = 1$ but $A = -1$ (sink-type configuration). The black region corresponds to the forbidden region. The sonic circle r_h is quasicoincident with the critical radius r_c so it has not be shown.

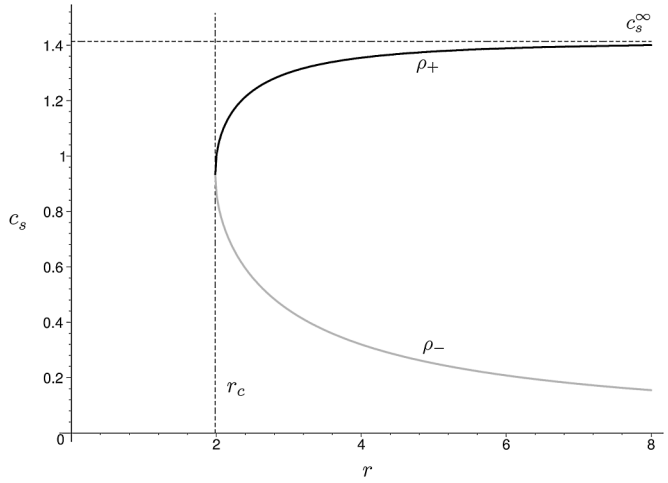

FIG. 5. Local sound speed versus radius r plot for the $n = 0.5$ solution with parameters $A = B = k = C_1 = 1$. The solution with the plus sign ρ_+ is in black while the ρ_- one is in gray with asymptotic value c_s^∞. The plot is the same for $A = -1$.

D. The case $n=1$

The $n = 1$ case leads for Eq. (13) to

$$\frac{4kr^2\rho^3 + (B^2 - 2C_1r^2)\rho^2 + A^2}{2r^2\rho^2} = 0. \tag{20}$$

The relation can be inverted by using standard algebra formulas for the roots of a third order polynomial. More in detail the transformation

$$\rho = \xi - \left(\frac{B^2 - 2C_1r^2}{12kr^2}\right) \tag{21}$$

casts our relation into the new form (depressed cubic)

$$\begin{aligned} &\xi^3 + P\xi + Q = 0, \qquad P = -\frac{(B^2 - 2C_1r^2)^2}{48k^2r^4}, \\ &Q = \frac{(B^2 - 2C_1r^2)^3}{864k^3r^6} + \frac{A^2}{4kr^2}, \end{aligned} \tag{22}$$

and from this point one can use standard algebra (Cardano formulas or others) to get the explicit form of the roots. We are not interested more in this case due to its quite lengthy mathematical expression. What matters here is that the solution practically behaves qualitatively as in the $n = 0.5$ case already studied with two roots $\rho_\pm$ and an U-shaped plot in the plane $\rho - r$. For this reason we shall not continue further its study.

E. Compressible flows in the isothermal limit $n \to +\infty$

Performing instead the $n \to +\infty$ isothermal limit in Eq. (12) we obtain

$$\left[k - \frac{A^2}{r^2\rho^2}\right]\frac{d\rho}{dr} - \frac{A^2}{r^3\rho} - \frac{B^2\rho}{r^3} = 0. \tag{23}$$

Integrating this we get

$$\rho(r) = \exp\left\{\frac{1}{2}\left[\mathcal{W}\left(-\frac{A^2\exp\left(\frac{B^2+2C_2r^2}{kr^2}\right)}{kr^2}\right) - \left(\frac{B^2 + 2C_2r^2}{kr^2}\right)\right]\right\}, \tag{24}$$

where C_2 is an integration constant and $y = \mathcal{W}(x)$ is the Lambert (or Product Log) function [28], solution of equation $ye^y = x$, and results complex for $x < -1/e$, while is real for bigger values. More in detail, it results negative if $x \geq -1/e$ with $\mathcal{W}(-1/e) = -1$ and positive for $x > 0$ [with $\mathcal{W}(0) = 0$]. This implies that our solution will exist for radii found by studying the inequality

$$-\frac{A^2\exp\left(\frac{B^2+2C_2r^2}{kr^2}\right)}{kr^2} \geq -\frac{1}{e} \tag{25}$$

which, using simple calculus arguments, implies that it can exist always a minimum radius, analytically given by

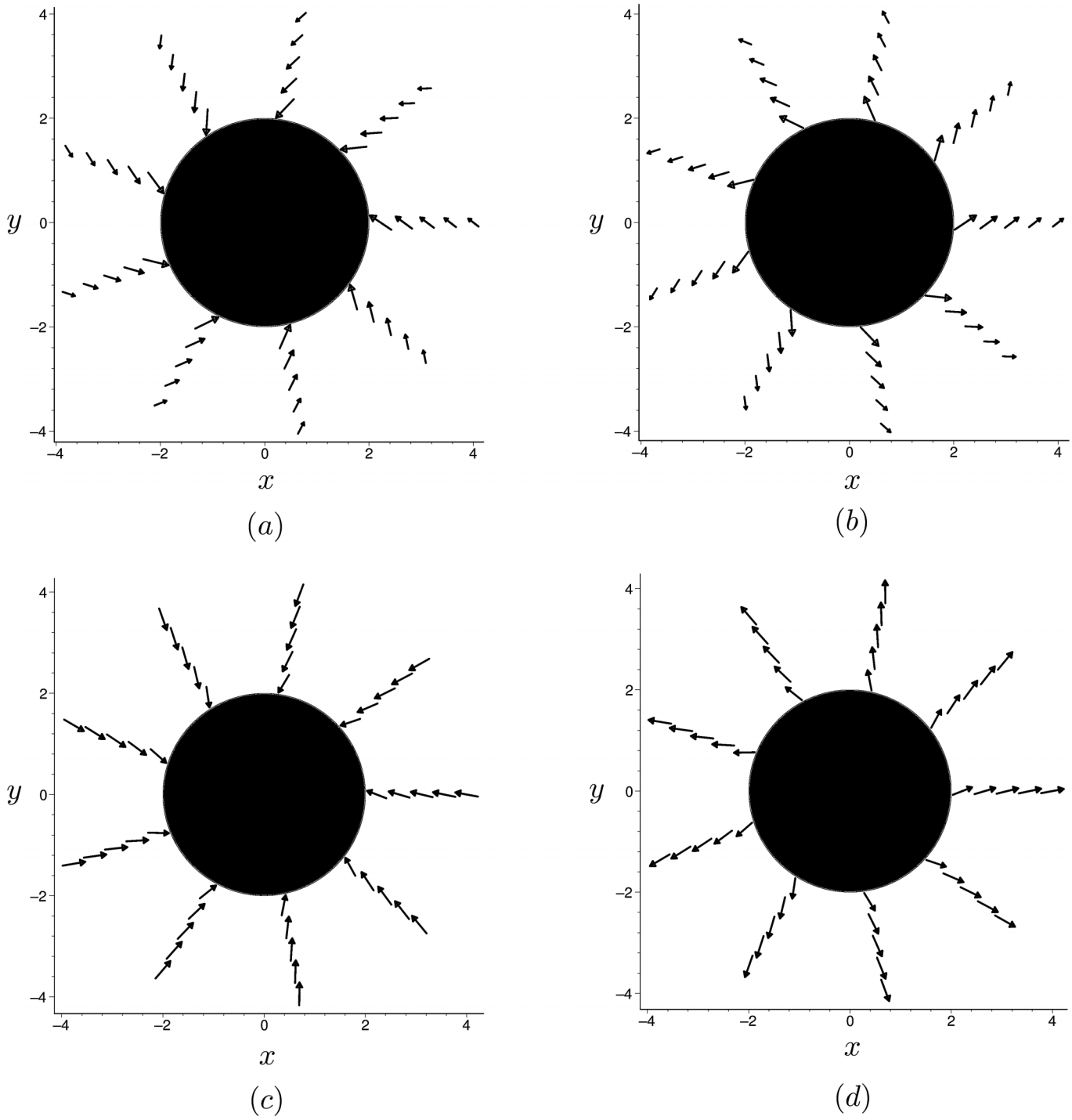

FIG. 6. Field plots for the $n = 0.5$ and parameters $B = k = C_1 = 1$ in the case: (a) ρ_+ and $A = -1$, (b) ρ_+ and $A = 1$, (c) ρ_- and $A = -1$, and (d) ρ_- and $A = 1$. Note the change of arrows' slope in the always supersonic branch ρ_- in comparison with the mixed case ρ_+.

$$r_c = \frac{B}{\sqrt{k\mathcal{W}(\frac{B^2}{A^2}e^{-(1+(2C_2/k))})}}, \tag{26}$$

beyond which a real solution fails to exist. At this critical radius, in any case, both the density and the velocity fields are regular. Finally, as expected from isothermal fluids physics, the speed of sound, given by Eq. (11) is constant and results in $c_s^2 = k$.

As in the previous case, we present here two plots which show, assuming $A = B = k = C_2 = 1$, the situation more in detail. In Fig. 8 we plot the density versus radius up to the critical radius. The density has an asymptotic value of

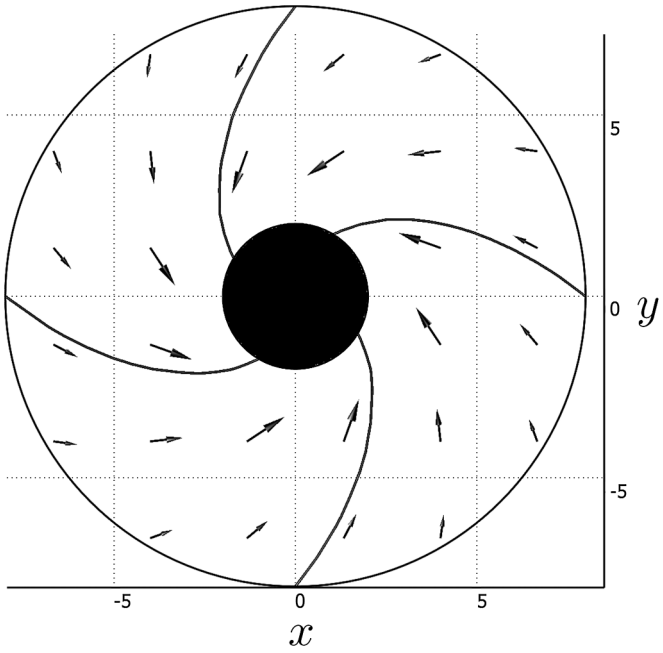

FIG. 7. Zoom of a circular region of the field lines with associated arrow plots for the $n = 0.5$ and ρ_+ solution with parameters $B = k = C_1 = 1$ and $A = -1$ (sink-type configuration). The black region corresponds to the forbidden region. The sonic circle r_h is quasicoincident with the critical radius r_c so in this plot it has not been shown. The plot in the case of the outgoing source type flux with $A = 1$ is analogous with the arrows pointing outside.

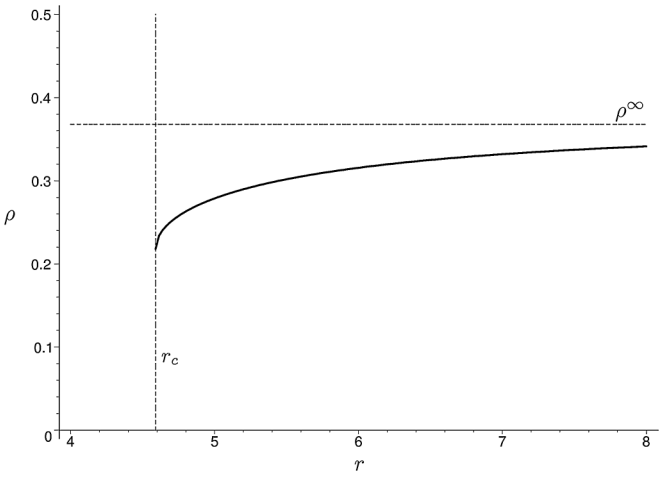

FIG. 8. Density ρ versus radius r plot for the isothermal $n \to +\infty$ solution with parameters $A = B = k = C_2 = 1$. The plot is the same in the case of the ingoing sink-type flux with $A = -1$.

$\rho^\infty = e^{-C_2}$ while at the critical radius r_c the density goes finite but with a complicated expression which is not relevant to be given here. The sonic radius r_s too has a complicated explicit form, so we shall consider the numerical plots only. In Fig. 9 instead we have the local Mach number $\mathcal{M}$ versus radius. Because of the constancy of the sound speed $c_s = \sqrt{k}$ from this plot we can immediately obtain the behavior of the magnitude of the velocity $v = |\vec{v}|$ as $v = \sqrt{k}\mathcal{M}$. The field lines and arrow plots for this configuration are qualitatively similar to the $n = 0.5$ already shown so we shall not plot them here again. The two distinct solution branches $\rho_\pm$ are not present (we have only the mixed case), but the behavior of this case is similar to the other two ones ($n = 0.5$ and $n = 1$) previously discussed. In the limit $r \to r_c$ one can show that again, as in the $n = 0.5$ case, the ratio $|v_r/c_s| = 1$.

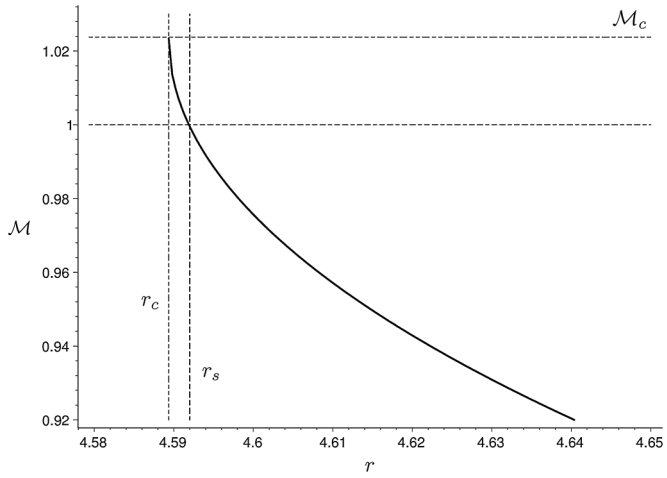

FIG. 9. Local Mach number $\mathcal{M}$ versus radius r zoomed plot for the isothermal $n \to +\infty$ solution with parameters $A = B = k = C_2 = 1$. At $r \to +\infty$ the speed goes to zero and so the Mach's number does. The plot is the same in the case of the ingoing sink-type flux with $A = -1$.

We point out a peculiar feature of the isothermal case. Assuming $A = 0$ in fact, i.e. an irrotational flow with no radial velocity component, the exact solution of Eq. (12) results in $\rho(r) = \rho_0 \exp[-B^2/(2kr^2)]$ with ρ_0 being a positive constant. This solution is well behaved for any radius although the velocity field is still pathological at $r = 0$. The presence of the "nonconventional" Lambert functions however prevents us to use the isothermal solution (24) in the following analysis of the acoustic metrics focusing instead on the $n = 0.5$ case, which, due to the very simple analytical form of the various expressions, is more amenable of an analytical study.

F. Negative polytropic indices: the case $n = -1$

Polytropic configurations can be defined also for negative polytropic indices. For a discussion of this physics we refer to Horedt monograph [27]. Here we analyze the $n = -1$ case only which, from the equation of state, leads to a constant pressure configuration, i.e. an isobaric regime. In this case Eq. (12) has the positive density solution

$$\rho = \frac{A}{\sqrt{C_1 A^2 r^2 - B^2}} \tag{27}$$

which has $c_s = 0$ and an infinite density at $r \to \frac{1}{\sqrt{C_1}} \frac{B}{A}$. It results nonphysical then so we do not consider it here together with the remaining negative polytropic index cases.

III. THE ACOUSTIC GEOMETRY

The acoustic analogy can be developed both for irrotational and rotational perfect fluid configurations. Its main outcome is that the perturbations of a perfect barotropic fluid can be rewritten in the form

$$\frac{1}{\sqrt{-g}} \partial_\mu (\sqrt{-g} g^{\mu\nu} \partial_\nu \Psi_1) = (\text{source terms}), \tag{28}$$

(here Greek indices run from 0 to 3) which is a scalar field equation on a curved four dimensional Lorentzian manifold called the acoustic metric, built with background hydrodynamical quantities, which are exact solutions of Euler's equations. If one studies irrotational configurations [4–6], then the field Ψ_1 is the perturbed velocity potential together with a zero source term. If instead rotation is present, the field Ψ_1 is a gauge invariant combination of background and perturbed quantities meaningful in the already mentioned Clebsch's potentials formalism, and the source term contains other dynamical variables to be coupled with additional differential equations coming from the perturbed hydrodynamics [18]. We do not explain here further all the details referring to the references listed above. What matters is that, in conclusion, for a generic nonviscous problem, the perturbations about an exact solution are essentially described through the acoustic metric tensor $g_{\mu\nu}$.

In particular, passing from Cartesian to cylindrical coordinates, the general acoustic line element of Ref. [6] results in

$$\begin{aligned} ds^2 &\equiv g_{\mu\nu} dx^\mu dx^\nu \\ &= \left(\frac{\rho}{c_s}\right)[-(c_s^2 - v^2)dt^2 - 2v_r dr dt - 2r v_\theta d\theta dt \\ &\quad - 2v_z dz dt + dr^2 + r^2 d\theta^2 + dz^2], \end{aligned} \tag{29}$$

where as usual $v = \sqrt{v_r^2 + v_\theta^2 + v_z^2}$. The inverse of the associated metric tensor is fundamental in order to understand the characteristics of the partial differential equation governing the evolution of perturbations [17,29].

We specialize the ds^2 given by Eq. (29), to our configuration in which all fields depend on radius r only with moreover $v_z = 0$. We can construct from the Riemann tensor $R_{\alpha\beta\gamma\delta}$ the Khretschmann invariant [30] for this line element $\mathcal{K} = R_{\alpha\beta\gamma\delta} R^{\alpha\beta\gamma\delta}$ in the case of the velocity field chosen in this article and insert then the solutions found for $n = 0.5$ discovering that $\mathcal{K} \to \infty$ for $r \to r_c$ in both cases, i.e. the last physical radius corresponds to an infinite curvature singularity. Monotonically this invariant decreases in the outgoing direction, having a finite value at the sonic radius r_s and then approaching zero at radial infinity for the ρ_+ branch. On the other hand the ρ_- branch has a nonflat asymptotic limit. The divergence is present clearly even if we work in a $2 + 1$ space-time suppressing the z dimension. In Fig. 10 we plot the logarithm to base 10 of this invariant. In Fig. 11 we perform the same study but for the isothermal case instead. We point out that in General Relativity, when a totally collapsed body (a Kerr black hole) is rotating, the curvature singularity is

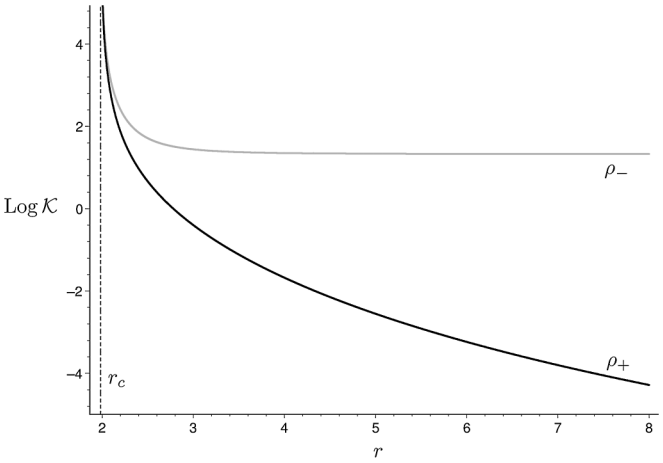

FIG. 10. Plot of Log$\mathcal{K}$ ($\mathcal{K}$ is Khretschmann curvature invariant) versus radius r for the $n = 0.5$ solution with parameters $A = B = k = C_1 = 1$ for the two branches ρ_+ and ρ_-. At critical radius r_c both of these go to infinity (curvature singularity). At radial infinity the ρ_+ branch leads to a vanishing value (asymptotic flat space-time) while the ρ_- one leads to a constant value (a nonflat situation). The plot is the same in the $A = -1$ case.

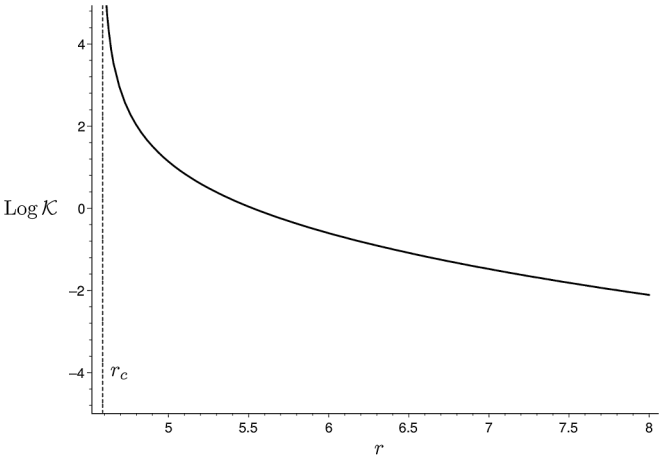

FIG. 11. Plot of Log$\mathcal{K}$ ($\mathcal{K}$ is Khretschmann curvature invariant) versus radius r for the $n \to +\infty$ (isothermal case) solution with parameters $A = B = k = C_2 = 1$. At critical radius r_c the invariant goes to infinity (curvature singularity). At radial infinity instead it leads to a vanishing value (asymptotic flat space-time). The plot is the same in the $A = -1$ case.

concentrated in a ring. We notice then that in this hydrodynamical case too a nonpointlike structure of the singularity occurs (this happens in two dimensions while in three dimensions, by extruding along the z direction, we have a cylindrically shaped singularity).

We can study now the null geodesics of the general class of acoustic space-times of Eq. (29) again, with pure radial dependence only for the hydrodynamical quantities and no v_z. The four-dimensional wave-vector $k^\alpha = dx^\alpha/d\lambda$ (λ is the affine parameter) satisfies the geodesic equations

$$\frac{dk^\alpha}{d\lambda} + \Gamma^\alpha_{\sigma\delta} k^\sigma k^\delta = 0, \tag{30}$$

but this vector must be also null i.e. $k^\alpha k_\alpha = 0$, so replacing $k_\alpha = \partial_\alpha S$ in the latter we obtain the eikonal equation

$$g^{\alpha\beta}\partial_\alpha S \partial_\beta S = 0. \tag{31}$$

The very simple Killing vectors structure of our acoustic metric, whose fields depend on radius only, allows us to adopt standard Hamilton-Jacobi treatment of geodesics commonly used in GR black hole physics [31–33].

We impose, for null (i.e. massless) geodesics

$$S(t, r, \theta, z) = -\mathcal{E}t + f(r) + \mathcal{L}\theta + \mathcal{Z}z, \tag{32}$$

where $\mathcal{E}$, $\mathcal{L}$, and $\mathcal{Z}$ are real constants.

Inserting in the eikonal equation we get

$$\underbrace{\frac{c_s^2 - v_r^2}{\rho c_s}}_{\alpha_1}\left(\frac{df}{dr}\right)^2 + \underbrace{\frac{2v_r(\mathcal{E}r - v_\theta \mathcal{L})}{\rho c_s r}}_{\alpha_2}\left(\frac{df}{dr}\right) + \underbrace{\left(\frac{c_s}{\rho r^2}\mathcal{L}^2 - \frac{(\mathcal{E}r - v_\theta\mathcal{L})^2}{\rho c_s r^2}\right)}_{\alpha_3} = 0. \tag{33}$$

This is a biquadratic equation which can be solved in terms of df/dr leading to the two differential equations

$$\frac{df}{dr} = -\frac{\alpha_2}{2\alpha_1} \pm \sqrt{\left(\frac{\alpha_2}{2\alpha_1}\right)^2 - \frac{\alpha_3}{\alpha_1}} \equiv k_r^\pm. \tag{34}$$

Something problematic here occurs when $\alpha_1 \to 0$, i.e. when $v_r \to c_s$ and our quadratic algebraic equation degenerates into a linear relation. This is Visser's condition which locates the event horizon in the acoustic draining bathtub but generalized here for more general compressible configurations.

From the initial considerations we have

$$k_\alpha^\pm = \partial_\alpha S \equiv \left(-\mathcal{E}, \frac{df}{dr}, \mathcal{L}, 0\right) = (-\mathcal{E}, k_r^\pm, \mathcal{L}, 0), \tag{35}$$

which, raised by $g^{\alpha\beta}$, gives the wave four-vectors $k_\pm^\alpha = k_\pm^\alpha(r)$ (for visual simplification only the $\pm$ in these expressions is bottom placed when we deal with vectors and vice versa for covectors.). If one is interested instead in the explicit world lines, from the very early definitions, the differential equations $\frac{dx^\alpha}{d\lambda} = k_\pm^\alpha$ must be numerically integrated. For the aims of our analysis however, we focus on the relation

$$\frac{\left(\frac{dr}{d\lambda}\right)}{\left(\frac{dt}{d\lambda}\right)} \equiv \frac{dr}{dt} = \frac{k_\pm^r}{k_\pm^t}, \tag{36}$$

where the affine parameter λ has disappeared. This equation gives the coordinate velocity for (not necessarily radial) null geodesic rays emanating at a certain initial space-time location. We have numerically integrated these equations in the $n = 0.5$ and ρ_+ case. We have moreover chosen $B = k = C_1 = 1$ and $A = \pm 1$ with geodesic parameters $\mathcal{E} = 1$, $\mathcal{L} = 0.5$, and $\mathcal{Z} = 0$. In Fig. 12 we plot the associated $r - t$ space-time diagram obtained in the sink-type configuration, while in Fig. 13 we have repeated the same plot but in the case of a source. As expected from standard black hole physics in horizon penetrating coordinates, on the horizon $r \to r_c$ we have $dr/dt \to 0$ or equivalently $dt/dr \to \infty$. The manifold in our analysis results moreover (null) geodesically incomplete [34,35]: the limiting circle (i.e. the singularity) in fact is reached at a finite affine parameter value.

We conclude our study focusing on the norm of the non-normalized (in general nongeodesic) Killing vector $\xi^\mu_{(t)} = (\partial/\partial t)^\mu$ given by

$$\xi^\mu_{(t)}\xi_{(t)\mu} = -\frac{\rho}{c_s}(c_s^2 - v_r^2 - v_\theta^2). \tag{37}$$

In our notations, using simple algebra, one case immediately verifies that this is timelike up to $r = r_s$. At this point

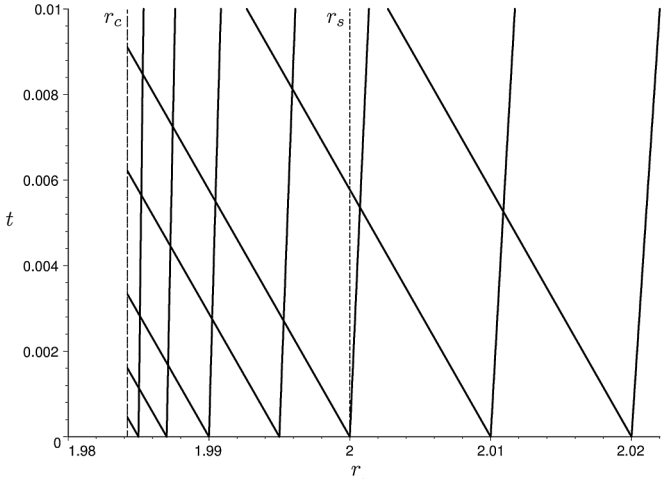

FIG. 12. Plot of the r-t space-time diagram for the geodesic light rays close to the critical region in the case $n = 0.5$, solution branch ρ_+ with $B = k = C_1 = 1$ and $A = -1$ (sink-type configuration). We have numerically integrated the equations choosing $\mathcal{E} = 1$, $\mathcal{L} = 0.5$, and $\mathcal{Z} = 0$. We point out the behavior close to r_c, where light rays bending approach what is expected to occur in an horizon penetrating coordinates black hole diagram of GR.

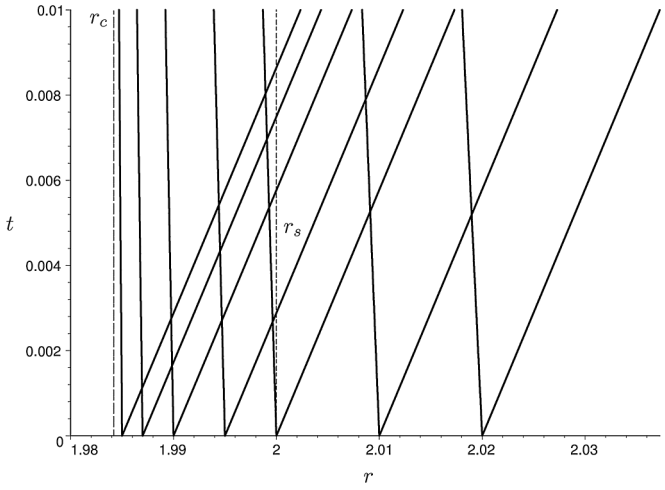

FIG. 13. Plot of r-t space-time diagram for the geodesic light rays close to the critical region in the case $n = 0.5$, solution branch ρ_+ with $B = k = C_1 = 1$ and $A = 1$ (source type configuration). We have numerically integrated the equations choosing $\mathcal{E} = 1$, $\mathcal{L} = 0.5$, and $\mathcal{Z} = 0$. We point out the behavior close to r_c, where light rays bending approach what is expected to occur in an horizon penetrating coordinates white hole diagram of GR.

it becomes lightlike and then spacelike up to the critical radius r_c. This shows that the radius r_s defines an ergosphere [32]. We have not considered in our study the ρ_- branch for $n = 0.5$. Because of its always supersonic nature in fact, its connection with GR is more delicate and consequently will be left to a future study. Qualitatively results very similar to the ones here discussed occur for the other physically interesting case of $n \to +\infty$ so we do not show then here the plots for this configuration too. The existence of a limit critical radius r_c for any index $n > 0$ suggests that also in the other not explicitly solvable cases a similar space-time structure must occur. These speculations too are left to be numerically confirmed by future studies however. We now discuss in the next section the physical implications of the results obtained.

IV. DISCUSSION

In an extremely simplified scenario of interest for classical gas dynamics [16], we have analytically observed that the stationary plane irrotational incompressible or compressible flows investigated are characterized by a critical radius beyond which solutions to gas dynamical field equations appear to be problematic. This radius cannot be identified as an obstacle: the matter density and fluid speed arrive in this limiting region with finite values so we expect that some of the initial *anzatz* adopted to derive the solution must break down there i.e. (1) irrotationality, (2) absence of gravity, (3) polytropic equation of state, and (4) no viscosity and heat transfer. Certainly in the inner region a different solution should exist to be matched with the exterior ones analyzed here, which however still continue to have physical relevance because in nature, as anticipated, rotating flows tend to manifest (see Fig. 1) a minimal radius beyond which zero (or small) fluid/matter is present.

What comes immediately in mind are, as an example, tornadoes, hurricanes and typhoons as well as the usual flows in a sink. Typical tornadoes can have the damage path (the thickness of the filamentlike structure) ranging from tens of meters up to around a kilometer for the most destructive ones. Their estimated maximum wind speed ranges from around 112 km/h up to around 640 km/h [36], but all of these figures remain below the sonic barrier (we recall that the sound speed in normal atmospheric conditions is around 340 m/s which corresponds to about 1200 km/h). In these cases an acoustic event horizon does not seem to be plausible to form then. We may try to speculate if in more extreme conditions, as in extraplanetary contexts, the sonic point could be reached. In Neptune's atmosphere is present a great dark spot which has diameter of around ten thousand kilometers and in this wind speeds are of around 700 km/h [37]. Regarding Jupiter, its big red spot is characterized by winds around the spot's edge at about 120 m/s, but currents inside it seem stagnant, with little inner or outer flows [38] (so our solution with $A \simeq 0$ would be more appropriate in this situation).

Summarizing, the common characteristic in each of these natural vortex systems is that they are all characterized by velocities below the speed of sound: the appearance of acoustic black holes seems difficult. On the other hand, man-made vortex structures can relatively easily be created both at low (subsonic) and high (supersonic/hypersonic) speeds. Typical situations of this type occur in high-speed missile and aircraft generated vortex flows (see Ref. [39] for a review) and in turbines and jets (see. Ref. [40] as an example). Standard methods adopted in fluid dynamics then should allow an experimentalist to observe if a perturbative acoustic wave is entirely absorbed by the system beyond a certain limit, i.e. if there exists an acoustic black hole and if, due to rotation, possibly superradiance [41], as already theoretically proven in the draining bathtub case [9,10,13,14,19,20,42], could occur here.

The presence of compressibility does not prevent one to look for possible applications of the theory here developed in the case of compressible quantum system. Typical examples can be trapped Fermi gases or Bose-Einstein condensates (BECs). In both of these systems a polytropic equation of state $p \propto \rho^{1+\gamma}$ can be adopted and their polytropic power $\gamma = 1/n$ can be fine tuned for different situations. As an example, in a dilute interaction dominated BEC, one obtains $\gamma = 1$, but for an ideal Bose gas in the normal state and under adiabatic conditions one gets $\gamma = 2/3$. Furthermore, a dilute Fermi atoms gas too, both in the hydrodynamic and superfluid limits, is characterized by the value above. Moreover, Fermi gases and BECs have $\gamma = 2/3$ in the strongly interacting limit, and

finally, near a Feshbach resonance, the (effective) power index γ ranges in $0.5 < \gamma < 1.3$ [43].

We remark again however that Euler's equations solutions found in this article, for any value of the polytropic index, break down at a certain radius, where, as we have seen, coordinate radial velocity of the simplest acoustic space-time perturbations (null geodesics) goes to zero while curvature blows up. The absence of a inner solution beyond this limit radius, strictly speaking, does not allow us to classify the configurations here studied as black holes, lacking of the possibility to have an inner region we cannot escape from. The presence of a curvature singularity exactly there, totally accessible by sound (in GR light) rays shows a marked difference in comparison with GR black holes and naked singularities. For this reason it appears mandatory to look for more general hydrodynamical solutions, which would allow us to explore the inner fluid region (if any). Because of the possible complications arising for analytical techniques, we consider fundamental then the construction and subsequent light cones inspection of the numerical acoustic metric tensors built from realistic three-dimensional numerical simulations of gas/fluid dynamics. To this aim the authors plan to address such studies in future adapting the numerical relativity methods developed previously in the case of the draining bathtub [11,12,14] on the lines of numerical experiments performed in the past in the simple case of the de Laval nozzle [15].

All of these perturbative studies however must be paralleled also by extended formulations of the acoustic metric at fully nonlinear hydrodynamical level [29,44]. Taking into account acoustic nonlinear waves, this will allow us to clarify the robustness of the analogy in real world and moreover better understand the appearance of black holes and curvature singularities at nonlinear level both in fluid dynamics and in General Relativity.

ACKNOWLEDGMENTS

The authors acknowledge ICRA and ICRANET for financial support.

APPENDIX

In this Appendix we show explicitly how to integrate analytically Eq. (12) for the generic positive index n. The existence of infinitesimal symmetry generators [45] given by $[\xi, \eta] = [(\rho^2 r^3)/(A^2 + \rho^2 B^2), 0]$ for our differential equation, suggests the introduction of the canonical coordinates transformation

$$z = \rho(r), \qquad s(z) = -\frac{A^2 + \rho(r)^2 B^2}{2r^2 \rho(r)^2} \tag{A1}$$

with associated inverse relations

$$\rho(r) = z, \qquad r = \pm \frac{1}{z}\sqrt{-\frac{A^2 + z^2 B^2}{2s(z)}}. \tag{A2}$$

Inserted into Eq. (12) by assuming positive sign because of the radius positivity, this simplifies to

$$\frac{ds(z)}{dz} = \frac{k(n+1)z^{(1/n)-1}}{n}, \tag{A3}$$

which can be immediately integrated leading to

$$s(z) = k(n+1)z^{1/n} - C_1, \tag{A4}$$

where C_1 is a generic integration constant. Inserting in Eq. (A4) the initial transformation (A1) we obtain the general solution (13).

[1] C. Barceló, S. Liberati, and M. Visser, Living Rev. Relativity **8**, 12 (2005).
[2] M. Novello, M. Visser, and G. E. Volovik, *Artificial Black Holes* (World Scientific, Singapore, 2002).
[3] W. Unruh and R. Schutzhold, *Quantum Analogues: From Phase Transitions to Black Holes and Cosmology*, Lecture Notes in Physics, Vol. 718 (Springer, Berlin, 2007).
[4] W. G. Unruh, Phys. Rev. Lett. **46**, 1351 (1981).
[5] W. G. Unruh, Phys. Rev. D **51**, 2827 (1995).
[6] M. Visser, Classical Quantum Gravity **15**, 1767 (1998).
[7] V. Cardoso, O. J. C. Dias, J. P. S. Lemos, and S. Yoshida, Phys. Rev. D **70**, 044039 (2004).
[8] E. Berti, V. Cardoso, and J. P. S. Lemos, Phys. Rev. D **70**, 124006 (2004).
[9] S. Basak and P. Majumdar, Classical Quantum Gravity **20**, 2929 (2003).
[10] S. Basak and P. Majumdar, Classical Quantum Gravity **20**, 3907 (2003).
[11] C. Cherubini, F. Federici, S. Succi, and M. P. Tosi, Phys. Rev. D **72**, 084016 (2005).
[12] F. Federici, C. Cherubini, S. Succi, and M. P. Tosi, Phys. Rev. A **73**, 033604 (2006).
[13] E. S. Oliveira, S. R. Dolan, and L. C. B. Crispino, Phys. Rev. D **81**, 124013 (2010).
[14] C. Cherubini and S. Filippi, J. Korean Phys. Soc. **56**, 1668 (2010).
[15] H. Furuhashi, Y. Nambu, and H. Saida, Classical Quantum Gravity **23**, 5417 (2006).
[16] R. Courant and K. O. Friedrichs, *Supersonic flow and shock waves* (Springer, New York, 1977).
[17] R. Von Mises, *Mathematical Theory of Compressible Fluid Flow* (Dover, New York, 2004).
[18] S. E. P. Bergliaffa, K. Hibberd, M. Stone, and M. Visser, Physica D (Amsterdam) **191**, 121 (2004).
[19] D. Bini, C. Cherubini, and S. Filippi, Phys. Rev. D **78**, 064024 (2008).

[20] D. Bini, C. Cherubini, S. Filippi, and A. Geralico, Phys. Rev. D **82**, 044005 (2010).
[21] D. Bini, C. Cherubini, and S. Filippi, Phys. Rev. D **83**, 064039 (2011).
[22] H. Lamb, *Hydrodynamics* (Dover, New York, 1993).
[23] T. Kambe, *Elementary Fluid Mechanics* (World Scientific, Singapore, 2007).
[24] A. Friedman, *Variational Principles and Free-Boundary Problems* (Dover, New York, 2010).
[25] R. B. Bird, W. E. Stewart, and E. N. Lightfoot, *Transport Phenomena* (Wiley, New York, 2002), 2nd edition.
[26] S. Chandrasekhar, *An Introduction to the Study of Stellar Structure* (Dover, New York, 1958).
[27] G. P. Horedt, *Polytropes, Applications in Astrophysics and Related Fields* (Kluwer Academic Publishers, Dordrecht, The Netherlands, 2004).
[28] R. M. Corless, G. H. Gonnet, D. E. G. Hare, D. J. Jeffrey, and D. E. Knuth, Adv. Comput. Math. **5**, 329 (1996).
[29] C. Cherubini and S. Filippi, ''Von Mises potential flow wave equation and nonlinear analog gravity'' Phys. Rev. D (2011) (unpublished).
[30] I. Ciufolini and J. A. Wheeler, *Gravitation and Inertia* (Princeton University, Princeton, NJ, 1995).
[31] L. D. Landau and E. M. Lifshitz, *The Classical Theory of Fields* (Butterwoth-Heineman, Oxford, 1975), 4th ed..
[32] V. Frolov and I. Novikov, *Black Hole Physics: Basic Concepts and New Developments* (Springer, New York, 1998).
[33] C. W. Misner, K. S. Thorne, and J. A. Wheeler, *Gravitation* (W. H. Freeman, New York, 1973).
[34] R. M. Wald, *General Relativity* (University of Chicago, Chicago, 1984).
[35] S. W. Hawking and G. F. R. Ellis, *The Large Scale Structure of Space-Time* (Cambridge University Press, Cambridge, England, 1973).
[36] M. Y. H. Bangash, *Shock, Impact and Explosion: Structural Analysis and Design* (Springer, New York, 2009).
[37] J. Daintith and W. Gould, *The Facts on File Dictionary of Astronomy* (Infobase Publishing, New York, 2006).
[38] J. H. Rogers, *The Giant Planet Jupiter* (Cambridge University Press, Cambridge, England, 1995).
[39] R. M. Wood, F. J. Wilcox, Jr., S. X. S. Bauer, and J. M. Allen, Report No. NASA/TP-2003-211950, 2003.
[40] A. Dauptain, B. Cuenot, and L. Y. M. Gicquel, AIAA J. **48**, 2325 (2010).
[41] J. D. Bekenstein and M. Schiffer, Phys. Rev. D **58**, 064014 (1998).
[42] F. Marino, M. Ciszak, and A. Ortolan, Phys. Rev. A **80**, 065802 (2009).
[43] H. Heiselberg, Phys. Rev. Lett. **93**, 040402 (2004).
[44] P. T. Chrusciel, in *The Conformal Structure of Space-Time: Geometry, Analysis, Numerics, Proceedings of the internationl workshop, Tübingen, Germany, 2001*, Lect. Notes Phys., edited by J. Frauendiener and H. Friedrich (Springer, Berlin, Germany, 2002), Vol. 604, p. 61.
[45] P. E. Hydon, *Symmetry Methods for Differential Equations: A Beginner's Guide* (Cambridge University Press, Cambridge, England, 2000).